Diamond & Related Materials 20 (2011) 1026–1029

Contents lists available at ScienceDirect

Diamond & Related Materials

journal homepage: www.elsevier.com/locate/diamond

Low-energy band structures of armchair ribbon-graphene hybrid systems☆☆

C.H. Lee [a], S.C. Chen [b], R.B. Chen [c], M.F. Lin [b,*]

[a] Institute of Applied Physics, National Chengchi University, Taipei City 116, Taiwan
[b] Department of Physics, National Cheng Kung University, Tainan 701, Taiwan
[c] Center of General Education, National Kaohsiung Marine University, Kaohsiung 811, Taiwan

ARTICLE INFO

Available online 22 June 2011

Keywords:
Graphene nanoribbons
Monolayer graphene
Electronic properties

ABSTRACT

The electronic properties of armchair ribbon-graphene hybrid systems are studied within the $2p_z$ tight-binding model. The geometric structures of graphene nanoribbons, such as the width (N_y) and the period (R_y) of the ribbons, greatly determine the band structures. Furthermore, the stacking arrangement between graphene nanoribbons and monolayer graphene also plays an important role in low-energy states. Energy gaps caused by AA- and AB-stacking are dependent on N_ys and R_ys differently. These geometric structure effects can be well identified by the density of states.

1. Introduction

The few-layer graphenes, which had been realized through mechanical friction [1] and thermal decomposition [2], are well-known two-dimensional (2D) carbon-related materials. Moreover, monolayer and bilayer graphenes also display unconventional quantum Hall effects in transport properties [3,4]. Theoretical investigations of the electronic properties of the two systems have been made by using the tight-binding model [5–7] and density functional theory [8,9]. It is found that the energy dispersion near the Fermi level (E_F) is sensitive to the stacking arrangement as well as the layer number.

The quasi-one-dimensional (Q1D) graphene nanoribbons could be regarded as the graphene patterned into a narrow ribbon. Such fascinating materials could be produced by many physical treatments and chemical synthesis [10–12]. They are usually termed the zigzag and armchair graphene nanoribbons, corresponding to the zigzag and armchair shaped edges, respectively. The finite width and edge configuration make the electronic properties of the graphene nanoribbon different from those of graphene. For instance, in the armchair ribbon, the band structures would depend on the width due to the quantum confinement and have also been studied and reported theoretically [13–16].

2. Theory

The geometric structure of an armchair ribbon-graphene hybrid system is shown in Fig. 1(a). This hybrid system consists of the ribbons aligned periodically along the y-axis on the graphene. The width of ribbons is N_y and the period is R_y, and they denote the number of the dimer lines. The interlayer distance between ribbon and graphene is assumed to be $c = 3.35$ Å, which is the same as that of the graphite. The C-C bond length is $b = 1.42$ Å. The unit cell of this system has $(2N_y + 2R_y)$ carbon atoms, and its lengths along the x-axis and y-axis are $I_x = 3b$ and $I_y = \left(\sqrt{3}b/2\right)R_y$, respectively. The first Brillouin zone is defined by $-\pi/I_x \le k_x \le \pi/I_x$ and $-\pi/I_y \le k_y \le \pi/I_y$.

Considering the tight-binding model with the $2p_z$-orbitals of the carbon atoms, the Hamiltonian matrix in the electric field could be represented as

$$H = \begin{pmatrix} h_1 & h_{12} \\ h_{12}^* & h_2 \end{pmatrix}.$$

The block h_1 is a $2N_y \times 2N_y$ Hamiltonian matrix of the armchair graphene nanoribbon, whereas h_2 is a $2R_y \times 2R_y$ Hamiltonian matrix of the monolayer graphene. The elements of the h_1 and h_2 with the AB-stacking are given by

$$\left(h_{ij}\right)_1 = \begin{cases} \gamma_6 & \text{if } j = i, \quad i \text{ is odd;} \\ \gamma_0 e^{i\left(k_x b/2 + k_y\sqrt{3}b/2\right)} & \text{if } j = i+3, \quad i \text{ is odd;} \\ \gamma_0 e^{-i\left(k_x b/2 - k_y\sqrt{3}b/2\right)} & \text{if } j = i+1, \quad i \text{ is even;} \\ \gamma_0 e^{-ik_x b} & \text{if } j = i+1, \quad i \text{ is odd} \\ 0 & \text{others,} \end{cases} \tag{1}$$

☆☆ Presented at the Diamond 2010, 21st European Conference on Diamond, Diamond- Like Materials, Carbon Nanotubes, and Nitrides, Budapest.

* Corresponding author.
E-mail address: mflin@mail.ncku.edu.tw (M.F. Lin).

0925-9635/$ – see front matter © 2011 Elsevier B.V. All rights reserved.
doi:10.1016/j.diamond.2011.06.008

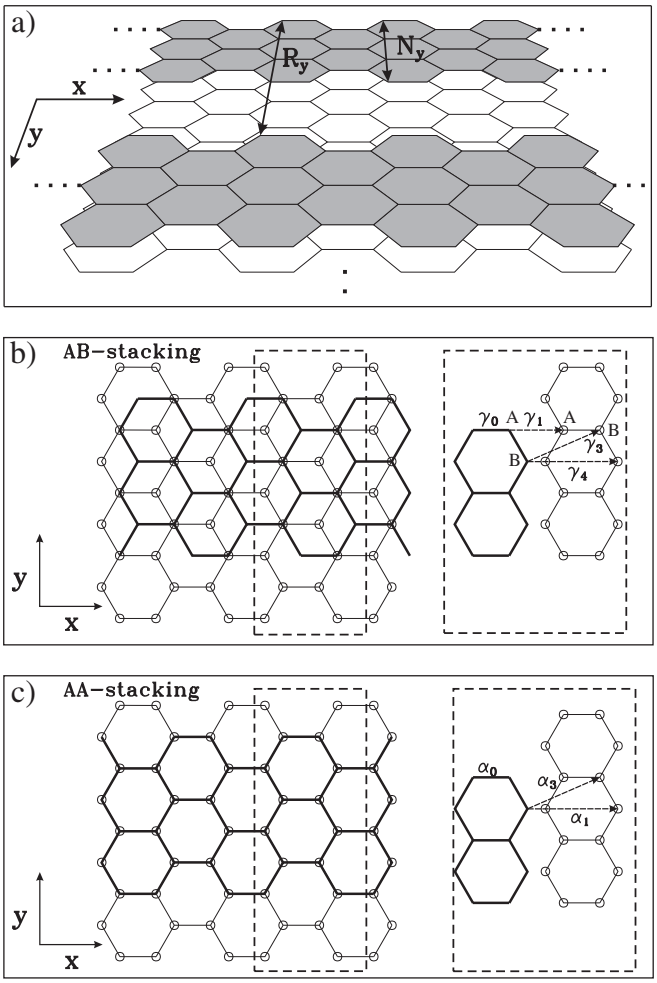

Fig. 1. (a) The geometric structure of an armchair ribbon-graphene hybrid system. N_y and R_y represent the ribbon width and period, respectively. (b) The ribbon is projected onto the graphene with the thick black lines in the AB-stacked hybrid system. γ_0 is the intralayer interaction and γ_is indicate the interlayer interactions. (c) same plot as (b), but shown for the AA-stacked hybrid system.

and

$$\left(h_{ij}\right)_2 = \begin{cases} \gamma_6 & \text{if } j=i, \quad i \text{ is even}, \ i<2N_y+4; \\ \gamma_0 e^{i\left(k_x b/2 + k_y\sqrt{3}b/2\right)} & \text{if } j=i+3, \quad i \text{ is odd}; \\ \gamma_0 e^{-i\left(k_x b/2 - k_y\sqrt{3}b/2\right)} & \text{if } j=i+1, \quad i \text{ is even}; \\ \gamma_0 e^{-ik_x b} & \text{if } j=i+1, \quad i \text{ is odd} \\ \gamma_0 e^{i\left(k_x b/2 - k_y\sqrt{3}b/2\right)} & \text{if } i=1, \ j=2R_y; \\ \gamma_0 e^{-i\left(k_x b/2 + k_y\sqrt{3}b/2\right)} & \text{if } i=2, \ j=2R_y-1; \\ 0 & \text{others}. \end{cases} \quad (2)$$

In this study, the armchair graphene nanoribbon and monolayer graphene are arranged according to Bernal (AB) stacking, as shown in Fig. 1(b). One atom (A atom) of the C-C bond is projected onto the A atom of the ribbon, and another (B atom) is projected onto the center of the hexagonal lattice. There exists a different value γ_6 between the on-site energies of A atom and B atom on the same layer due to the AB manner. In the ribbon (graphene), the A atom corresponds to the ith atom in which i equals odd integer (even integer).

In the h_{12}, the interactions of the $2p_z$ orbitals between the graphene nanoribbon and monolayer graphene with AB-stacking could be expressed by

$$\left(h_{ij}\right)_{12} = \begin{cases} \gamma_4 e^{-i\left(k_x b/2 + k_y\sqrt{3}b/2\right)} & \text{if } j=i, \quad i \text{ is odd}; \\ \gamma_4 e^{ik_x b} & \text{if } j=i+2, \quad i \text{ is odd}; \\ \gamma_4 e^{-i\left(k_x b/2 - k_y\sqrt{3}b/2\right)} & \text{if } j=i+4, \quad i \text{ is odd}; \\ \gamma_1 & \text{if } j=i+3, \quad i \text{ is odd} \\ \gamma_4 e^{-i\left(k_x b/2 + k_y\sqrt{3}b/2\right)} & \text{if } j=i, \quad i \text{ is even}; \\ \gamma_4 e^{-ik_x b} & \text{if } j=i+2, \quad i \text{ is even}; \\ \gamma_4 e^{-i\left(k_x b/2 - k_y\sqrt{3}b/2\right)} & \text{if } j=i+4, \quad i \text{ is even}; \\ \gamma_3 e^{i\left(k_x b/2 - k_y\sqrt{3}b/2\right)} & \text{if } j=i-1, \quad i \text{ is even}; \\ \gamma_3 e^{-ik_x b} & \text{if } j=i+1, \quad i \text{ is even}; \\ \gamma_3 e^{i\left(k_x b/2 + k_y\sqrt{3}b/2\right)} & \text{if } j=i+3, \quad i \text{ is even}; \\ 0 & \text{others}, \end{cases} \quad (3)$$

γ_0s and γ_is indicate the intralayer interactions and the interlayer interactions, respectively. That is, $\gamma_0 = 2.598$ eV, $\gamma_1 = 0.364$ eV, $\gamma_3 = 0.319$ eV, $\gamma_4 = 0.177$ eV, and $\gamma_6 = -0.026$ eV, corresponding to the values of the AB-stacked graphite [17].

Another arrangement in this hybrid system is the simple hexagonal (AA) stacking, as plotted in Fig. 1(c). In such a AA-stacking, all carbon atoms of the ribbon are projected directly onto those of the graphene. The corresponding intralayer and interlayer Hamiltonian elements can be expressed as follows:

$$\left(h_{ij}\right)_1 = \begin{cases} \alpha_0 e^{-ik_x b} & \text{if } j=i+1, \quad i \text{ is odd}; \\ \alpha_0 e^{i\left(k_x b/2 + k_y\sqrt{3}b/2\right)} & \text{if } j=i+3, \quad i \text{ is odd}; \\ \alpha_0 e^{-i\left(k_x b/2 - k_y\sqrt{3}b/2\right)} & \text{if } j=i+1, \quad i \text{ is even}; \\ 0 & \text{others}, \end{cases} \quad (4)$$

$$\left(h_{ij}\right)_2 = \begin{cases} \alpha_0 e^{-ik_x b} & \text{if } j=i+1, \ i \text{ is odd}; \\ \alpha_0 e^{i\left(k_x b/2 + k_y\sqrt{3}b/2\right)} & \text{if } j=i+3, \ i \text{ is odd}; \\ \alpha_0 e^{-i\left(k_x b/2 - k_y\sqrt{3}b/2\right)} & \text{if } j=i+1, \ i \text{ is even}; \\ \alpha_0 e^{i\left(k_x b/2 - k_y\sqrt{3}b/2\right)} & \text{if } i=1, j=2R_y; \\ \alpha_0 e^{-i\left(k_x b/2 + k_y\sqrt{3}b/2\right)} & \text{if } i=2, j=2R_y-1; \\ 0 & \text{others}, \end{cases} \quad (5)$$

and

$$\left(h_{ij}\right)_{12} = \begin{cases} \alpha_3 e^{i\left(k_x b/2 - k_y\sqrt{3}b/2\right)} & \text{if } j=i+3, \ i \text{ is odd}; \\ \alpha_3 e^{-i(k_x b} & \text{if } j=i+5, \ i \text{ is odd}; \\ \alpha_3 e^{i\left(k_x b/2 + k_y\sqrt{3}b/2\right)} & \text{if } j=i+7, \ i \text{ is odd}; \\ \alpha_1 & \text{if } j=i+4, \\ \alpha_3 e^{-i\left(k_x b/2 + k_y\sqrt{3}b/2\right)} & \text{if } j=i+1 \ i \text{ is even}; \\ \alpha_3 e^{i(k_x b} & \text{if } j=i+3, \ i \text{ is even}; \\ \alpha_3 e^{-i\left(k_x b/2 - k_y\sqrt{3}b/2\right)} & \text{if } j=i+5, \ i \text{ is even}; \\ 0 & \text{others}. \end{cases} \quad (6)$$

The hopping integrals α_0, α_1, and α_3 are taken from the simple hexagonal graphite in ref. [17]. By diagonalizing the Hamiltonian matrix, energy dispersion $E^{c,\,v}$ can be obtained, with the superscripts c and v representing the conduction π band and valence π band, respectively.

3. Results

Fig. 2(a) shows the band structures of the armchair ribbon-graphene hybrid system ($N_y = 18$, $R_y = 300$) along R-Y-Γ-X with $\Gamma(k_x = 0, k_y = 0)$, X$(\pi/\mathrm{I_x}, 0)$, Y$(0, \pi/\mathrm{I_y})$, and R$(\pi/\mathrm{I_x}, \pi/\mathrm{I_y})$. We only aim for the low-energy band structures for $k_x < 0.05$ 1/Å $\sim 0.068\,\pi/I_x$, and π/I_y is about one-sixth of 0.05 1/Å for $R_y = 300$. For the independent system, the low-energy band structures consist of the linear bands and

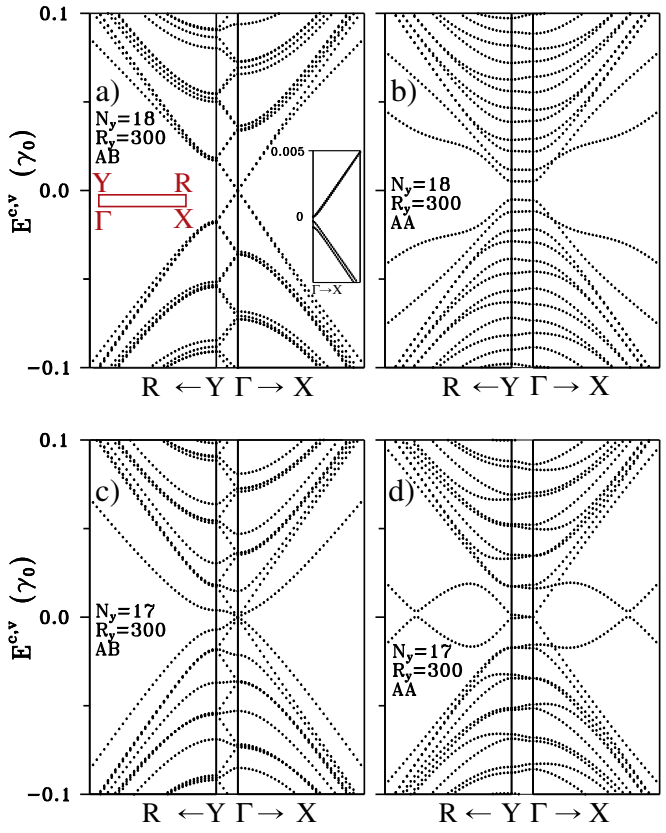

Fig. 2. The energy dispersion of the armchair ribbon-graphene system for $N_y=18$ and $R_y=300$ with (a) AB-stacking as well as (b) AA-stacking. The left inset in (a) is the one-fourth of rectangular first Brillouin zone with $\Gamma(0,0)$, $X(\pi/I_x,0)$, $Y(0,\pi/I_y)$, and $R(\pi/I_x,\pi/I_y)$. $I_x=3b$ and $I_y=\left(\sqrt{3}b/2\right)R_y$. The right inset in (a) shows the energy gap near E_F at Γ point. (c) and (d) are the same plots as (a) and (b), but for $N_y=17$.

parabolic bands, stemming from the single-layer graphene. In addition, the parabolic bands from the $N_y=18$ armchair ribbons appear near $\pm 0.1\gamma_0$. According to $R_y=3i$ (i an integer), the intersection of the linear bands from the single-layer graphene will be folded at the Γ point. With the consideration of the interlayer interactions of AB-stacking, the band structures would be slightly modified, as shown in Fig. 2(a). A narrow energy gap emerges at the Γ point (the right inset of Fig. 2(a)). The occurrence of the energy gap results from the energy difference between A and B atoms of the graphene with the AB-stacking. As k_x shifts slightly away from Γ, the linear bands would be gradually influenced by the ribbon. The energy dispersion would be modified and the corresponding tight-binding functions would vary with the atom sites. The band structures at Y point are different from that at Γ point. It means that the k_y dependence of band structure is still strong, similar to the single-layer graphene [18,19]. However, the AB-stacking would break the two-fold degeneracy at $k_y=0$ and $k_y=\pi/I_y$, and induce new band-edge states.

In Fig. 2(b), the low-energy band structures of the AA-stacked hybrid system are different from those of the AB-stacked one. In this system ($N_y=18$, $R_y=300$), the bands near the Fermi level would be altered and their dispersion would be reduced away from the $k_x=0$. Moreover, the gap is larger than the gap in the AB-stacked hybrid system. The difference between the energy bands along the k_x at $k_y=0$ and $k_y=\pi/I_y$ is small; that is, the k_y dependence of energy dispersions is weak in the AA-stacked hybrid system. The dispersionless feature can also be observed in the monolayer graphene under the modulated external fields [20]. It could be supposed that the interactions of the periodic ribbon on the graphene with AA-stacking have the similar effects.

Considering $N_y=17$ ribbon, there exist bands near Fermi level owing to the quantum confinement, and they are subjected to the interlayer interactions. In Fig. 2(c), the band structures of AB-stacked ($N_y=17$, $R_y=300$) are similar to those of ($N_y=18$, $R_y=300$) except the band structures near $E_F=0$. The three-fold degeneracy occurs at the Γ point and the energy gap vanishes. In addition, the bands near E_F from the armchair ribbon would significantly affect those from the single-layer graphene. There are two kinds of band modification along k_y. One remains linear to k_y, and the other is a weaker dispersion along the k_y.

In the AA-stacking, the k_y dependence of band structure with $N_y=17$ is also weak. However, the new band-edge states occur at low energy, as shown in Fig. 2(d). The band-edge states that disappear in the $N_y=18$ overlap nearly at $k_y=0$ and $k_y=\pi/I_y$. It could be found that their contributions come from the ribbons. In this system, the energy gap disappears and band crossing occurs between $k_y=0$ and $k_y=2\pi/3I_y$.

The characteristics of the band structures for such a hybrid system can be clearly presented in the density of states (DOS). The definition of DOS is given by

$$D(\omega)=\frac{2I_xI_y}{2\left(N_y+R_y\right)}\times \sum_{h=c,v}\int_{1stBZ}\frac{dk_xdk_y}{4\pi^3}\frac{\Gamma}{\left[\left(E^h\left(k_x,k_y\right)-\omega\right)^2+\Gamma^2\right]}. \tag{7}$$

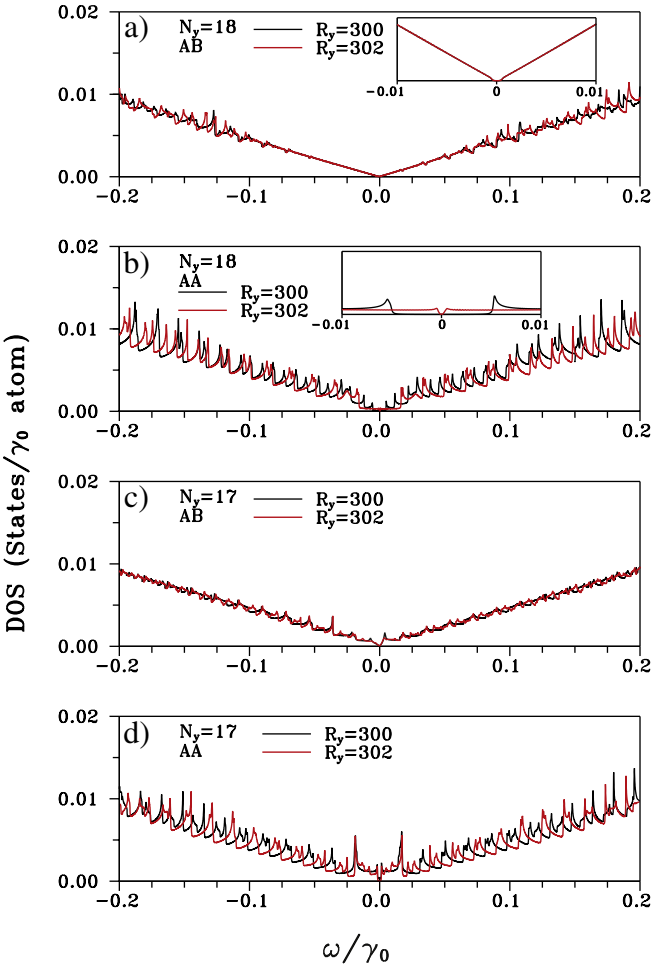

Fig. 3. Density of states (DOS) is calculated for $N_y=18$ armchair ribbons with the period $R_y=300$ and $R_y=302$ in (a) AB-stacking and (b) AA-stacking. (c) and (d) are the same plots as (a) and (b), but for $N_y=17$. The insets in (a) and (b) show the energy gap near E_F.

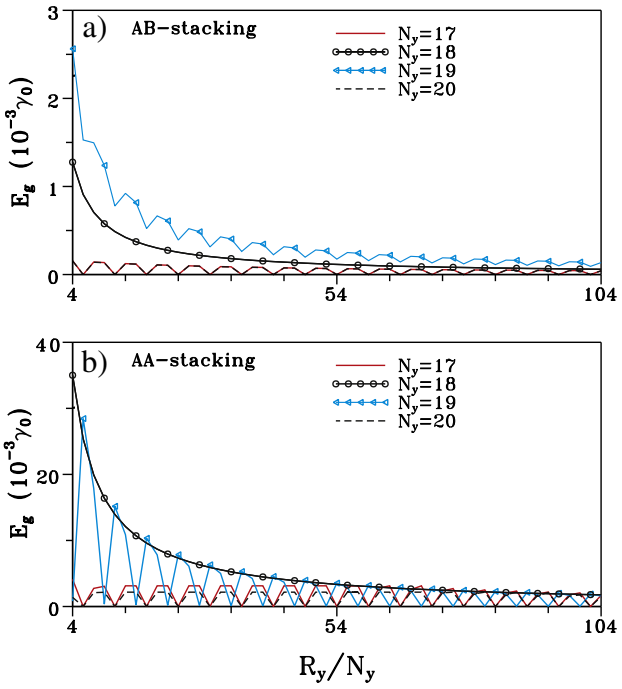

Fig. 4. The R_y-dependent energy gaps of the hybrid system for different N_ys with (a) AB- and (b) AA-stacking.

Γ ($=10^{-4}\gamma_0$) is the phenomenological broadening parameter. The DOSs of the $N_y=18$ with two periods $R_y=300$ and $R_y=300$ show similar behavior at low frequency ($\omega\leq||0.75\gamma_0||$), as shown in Fig. 3(a). Like the 2D graphene, DOSs do not exist at $\omega=0$, but they increase linearly as frequency raises. Small peaks occur owing to the band-edge states induced by the interlayer interactions. When the frequency is over $\pm0.1\gamma_0$, the peaks with the nearly square-root divergency appear because of the effects of the states from $N_y=18$ ribbons. In comparison, the DOS of AA-stacked hybrid systems would display obvious 1D structures even at low frequency, and means that the k_y dependence is reduced (Fig. 3(b)). The energy gap appears in the ($N_y=18$, $R_y=300$). When the period is changed to 302, E_g decreases and the peak frequencies vary. In addition, DOS of the $N_y=17$ hybrid system exhibits a distinct structure different from that of the $N_y=18$, as shown in Fig. 3(c). The amplitude of DOS at $\omega=0$ is still zero in spite of the vanishing of the energy gap. There exist stronger Q1D peaks at low energy, and they derive from the energy bands of the $N_y=17$ armchair GNR. The effects are also observed in the AA-stacked hybrid systems in Fig. 3(d).

The energy gap of the hybrid could be influenced by adjusting R_y/N_y with different N_ys. In Fig. 4(a), the hybrid systems in AB-stacking consisting of $N_y=17$ or $N_y=20$ armchair ribbons own smaller gaps. Meanwhile, E_g disappears and the linear bands of single-layer graphene intersect at the Γ point as R_y is the multiple of the three. As R_y varies, the magnitudes of E_g would be altered drastically. For $N_y=19$ and $N_y=18$, the gaps decrease with the increasing ribbon period. When $R_y=3i$ the gap is smaller than those for other values of R_y, and similar behavior of the gaps is observed for $N_y=17$ and $N_y=20$. The energy gaps of the AA-stacked system as a function of the ribbon's period would be different from those of the AB-stacked one and have larger values, as presented in Fig. 4(b). In case of $N_y=17$ and 20, the gap still disappears with $R_y=3i$ (i an integer) between $k_y=0$ and $k_y=2\pi/3I_y$. The gap would be constant in moderate R_y because the new edge state occurs along the k_x at $k_y=0$. The energy spacing between the new edge states would not be influenced by the ribbon's period, mainly owing to the energy band from the $N_y=17$ and 20 ribbons. However, the $N_y=18$ and $N_y=19$ exhibit different behavior with R_y. They could be classified into three groups, but the smaller gap does not occur at $R_y=3i$. For example, $N_y=18$ owns a smaller gap at $R_y=300$ than at $R_y=302$, as shown in the inset of Fig. 3(b). On the other hand, the smaller gaps of the $N_y=19$ locate at $R_y=3i+2$.

4. Conclusion

The electronic properties of the hybrid system are affected by the width and the period of ribbon, as well as the stacking types. The band structure of the AB-stacked system would be changed slightly by the interlayer interactions. In contrast, the AA-stacking would reduce the k_y dependence and induce more band-edge states along k_x. Moreover, E_g could be modified by varying N_y and R_y. The above-mentioned changes in the band structures could also be observed in DOS, such as the occurrence of quasi-one-dimensional peaks. These effects of the width and the period could be verified by the optical and transport experiments.

Acknowledgments

This work was supported by the NSC and NCTS of Taiwan, under the grant nos. NSC 98-2112-M-182-002-MY3 and NSC 98-2112-M-006-013-MY4.

References

[1] K.S. Novoselov, A.K. Geim, S.V. Morozov, D. Jiang, Y. Zhang, S.V. Dubonos, I.V. Grigorieva, A.A. Firsov, Science 306 (2004) 666.
[2] C. Berger, Z.M. Song, T.B. Li, X.B. Li, A.Y. Ogbazghi, R. Feng, Z.T. Dai, A.N. Marchenkov, E.H. Conrad, P.N. First, W.A. de Heer, J. Phys. Chem. B 108 (2004) 19912.
[3] Y. Zhang, Y.W. Tan, H.L. Stormer, P. Kim, Nature (London) 438 (2005) 201.
[4] K.S. Novoselov, E. McCann, S.V. Morozov, V.I. Fal'ko, M.I. Katsnelson, U. Zeitler, D. Jiang, F. Schedin, A.K. Geim, Nat. Phys. 2 (2006) 177.
[5] B. Partoens, F.M. Peeters, Phys. Rev. B 74 (2006) 075404.
[6] C.L. Lu, C.P. Chang, Y.C. Huang, R.B. Chen, M.L. Lin, Phys. Rev. B 73 (2006) 144427.
[7] J.H. Ho, C.L. Lu, C.C. Hwang, C.P. Chang, M.F. Lin, Phys. Rev. B 74 (2006) 085406.
[8] S.B. Trickey, F. Müller-Plathe, G.H.F. Diercksen, Phys. Rev. B 45 (1992) 4460.
[9] S. Latil, L. Henrard, Phys. Rev. Lett. 97 (2007) 036803.
[10] M. Murakami, S. Iijima, S. Yoshimura, J. Appl. Phys. 60 (1986) 3856.
[11] L. Jiao, L. Zhang, X. Wang, G. Diankov, H. Dai, Nature (London) 458 (2005) 877.
[12] K. Kim, A. Sussman, A. Zettl, ACS Nano 4 (2010) 1362.
[13] K. Nakada, M. Fujita, G. Dresselhaus, M.S. Dresselhaus, et al., Phys. Rev. B 54 (1996) 17954.
[14] K. Harigaya, Chem. Phys. Lett. 340 (2001) 123.
[15] F.L. Shyu, M.F. Lin, J. Phys. Soc. Jpn. 69 (2000) 3529.
[16] C.P. Chang, Y.C. Huang, C.L. Lu, J.H. Ho, T.S. Li, M.F. Lin, Carbon 44 (2006) 508.
[17] J.C. Charlier, J.-P. Michenaud, X. Gonze, Phys. Rev. B 46 (1992) 4531.
[18] J.H. Ho, Y.H. Lai, S.J. Tsai, J.S. Hwang, C.P. Chang, M.F. Lin, J. Phys. Soc. Jpn. 75 (2006) 114703.
[19] Y.H. Lai, J.H. Ho, C.P. Chang, M.F. Lin, Phys. Rev. B 77 (2008) 085426.
[20] J.H. Ho, Y.H. Chiu, S.J. Tsai, M.F. Lin, Phys. Rev. B 79 (2009) 115427.